Photoacoustic signal in strongly luminescent crystals: Bulk-surface states deexcitation model

M. Grinberg, A. Sikorska, and A. Śliwiński
Institute of Experimental Physics, University of Gdańsk, Wita Stwosza 57, 80-952 Gdańsk, Poland
(Received 23 May 2002; published 31 January 2003)

We present a model describing the photoacoustic-photothermal signal in the presence of spatial energy migration from the luminescence center to the surface. We have developed a quantitative model describing nonradiative internal conversion processes in the centers and energy migration in the sample and influence of both on the amplitude and phase of the photoacoustic signal. The model has been used for obtaining a relation between photoacoustic and absorption spectra in the yttrium aluminum garnet (YAG):Cr^{3+} crystal. We have estimated the local quantum efficiency of the Cr^{3+} in YAG and the quantity of the excitation energy diffusion length.

DOI: 10.1103/PhysRevB.67.045114 PACS number(s): 71.55.Ht, 76.30.Fc

I. INTRODUCTION

In standard theory of photoacoustic signal (PAS) generation[1] it is usually assumed that heat deposited at any particular location in the samples is derived only from the light absorbed at the same location. It is a good assumption when spatial migration of the excitation energy is negligible. As has been discussed in our previous paper[2] (paper I) in such a case the photoacoustic spectrum, defined as the dependence of PAS amplitude on excitation wavelength (or energy), is proportional to the absorption spectrum. The coefficient of proportionality is considered as the relative optical to thermal energy conversion efficiency. In this paper we focus our attention on the case where the excitation energy absorbed by a localized center after fast relaxation to the metastable excited state is transferred from the center to the surface states and then released as heat.

The effect of spatial energy migration in the solid state is quite well known. The physical background for the nonradiative transfer from point sensitiser to point activator has been examined by Dexter[3] and reexamined by Inokuti and Hirayama.[4] They have listed the mechanisms responsible for the energy transfer, namely, electric dipole, electric quadruple, and superexchange interactions. Later the model of energy transfer based on the diffusion effect was proposed.[5,6] The theory of transfer has been successfully used by many authors for describing the luminescence kinetics of sensitizers.[7–11] From our point of view the important conclusion is that the characteristic distance of sensitization depends on the interaction and can even extend up to 10^3 lattice constants.[3] In the case when energy migration between sensitizers is considered this distance can be much longer.[11]

Generation of PAS in the presence of spatial energy migration has been discussed theoretically by Quimby and Yen.[12] They analyzed the dependence of magnitude and phase of the PAS related to localized centers on modulation frequency exciting light. Flaherty and Powell[13] discussed the problem of concentration luminescence quenching for Nd^{3+} ions in $Nd_xY_{1-x}P_5O_{14}$ crystals. They presented a model that allowed one to calculate the probability of migration of the excitation to the surface for a given location of sensitizer. Although they measured and analyzed the PAS spectra, the influence of surface quenching on the PAS amplitude has not been discussed.

Our intuition regarding the photoacoustic effect is that that the nonradiative energy transfer becomes important and can influence the PAS of the system when the excitation deposited in the luminescence center is nonradiatively transferred within a distance larger than thermal diffusion length. We have considered that in such a case the simple relations between the characteristic absorption coefficient and PAS spectra are not valid and PAS, as well as other photothermal techniques need special treatment to yield the absorption spectrum of the system.

In paper I we have analyzed photoacoustic and absorption spectra of $Y_3Al_5O_{12}$ (YAG) doped with chromium and magnesium. We have found that in the as-grown sample and the sample annealed in air (part of the Cr^{3+} ions were oxidized to the Cr^{4+}), the relation between PAS and absorption can be easily explained by considering only the intracenter nonradiative relaxation. However, in the case when the material contains only octahedrally coordinated Cr^{3+} centers (in the sample annealed in hydrogen) the relation between the PAS and absorption cannot be described by the model of the relaxation process that neglects the excitation energy migration. Since in this case the first excited state of the Cr^{3+} system ^2E is the metastable state characterized by the lifetime equal to 3 ms we expect that the system is excited for a sufficiently long time to allow the process of migration of the excitation energy between the Cr^{3+} ions as well as from the Cr^{3+} to the surface.

The main purpose of the paper is to explain the relation between PAS and absorption spectra. We also consider the possibilities of using photoacoustic and photothermal methods for analysis of the spatial energy migration in the system.

II. PAS SIGNAL GENERATION

According to Rosencwaig Gersho[1] the PAS is proportional to the temperature of the sample surface that is calculated by solving thermal conductivity equation. We have assumed that the heat propagates in the sample in one direction z. The geometry of the sample with respect to the incident light beam is presented in Fig. 1. One neglects the heat emission at the sides of the sample [three-dimensional (3D) ef-

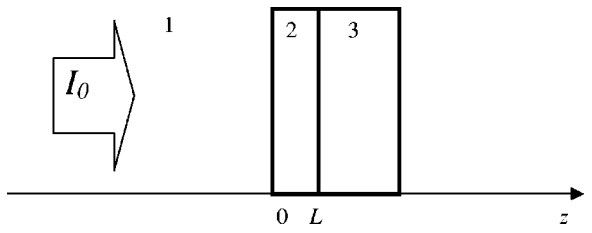

FIG. 1. Geometry of the system.

fect] when the sample thickness L is small in comparison to its diameter. This condition is satisfied in our case since sample diameter was 6 mm and thickness 1 mm. Under homogeneous excitation (it is assumed that the incident light is parallel to the z direction) the heat flow is described by the following equation:[14]

$$\frac{\partial^2\Theta(z,I)}{\partial z^2}-\frac{1}{\alpha}\frac{\partial\Theta(z,t)}{\partial t}=-\frac{\mathbf{H}(z,t)}{q}, \tag{1}$$

where $\Theta(z,t)$ is the temperature field, $\mathbf{H}(z,t)$ is the rate of heat input per unit volume, and α and q are the thermal diffusivity and conductivity, respectively. Considering only the harmonic part of the excitation with frequency ω one can replace Eq. (1) by

$$\frac{\partial^2T(z)}{\partial z^2}+\sigma^2T(z)=-\frac{H(z)}{q}, \tag{2}$$

where $\mathbf{H}(z,t)$ and $T(z)$ are defined as follows: $\mathbf{H}(z,t)=H(z)\exp(i\omega t)$ and $\Theta(z,t)=T(z)\exp(i\omega t)$. Quantity σ is related to thermal diffusion length $\lambda(\omega)=\sqrt{2\alpha/\omega}$ as follows: $\sigma=(1+i)/\lambda(\omega)$. Equation (2) can be solved using the Fourier transform $H(k)=\int H(z)\exp(-ikz)dz$,

$$T(z)=\frac{1}{2\pi}\int\frac{H(z)e^{ikz}dz}{q(k^2+\sigma^2)}+\theta e^{-\sigma z}+\phi e^{\sigma z}. \tag{3}$$

Constants θ and ϕ can be found from boundary conditions for temperature and thermal flux. We have considered three regions (see Fig. 1). The region for $-\infty<z<0$ corresponds to the air in front of the sample (we indicated this region as "1"). The region $0\leqslant z\leqslant L$ is related to the sample (we indicated this region as "2"). The third region is defined for $L\leqslant z<\infty$ (we indicated this region as "3"). Depending on the construction of the cell the third region can be the air or the background material. In our case it is the quartz window. Assuming that the heat is released only in the sample one can assume $H(z)=0$ in air and background material (regions 1 and 3).

One has to consider that the sample contains two types of states the bulk states of density $N_b(z)$ that contribute to the heat through $H_b(z)=N_b(z)Q_b$ and surface states N_{s1} and N_{s2} that contribute to the heat through $H_s=[N_{s1}\delta(z)+N_{s2}\delta(z-L)]Q_s$. Q_b and Q_s are the energies emitted as heat per individual process of deexcitation in the bulk material and at the surface, respectively. Considering that the bulk states are excited by absorption of photons of energy E one obtains

$$H(z)=H_b(z)+H_s(z)=C_be^{-\beta(E)z}+C_{s1}\delta(z)+C_{s2}\delta(z-L), \tag{4}$$

where $\beta(E)$ is optical absorption. Coefficients C_b, C_{s1}, and C_{s2} can also depend on the absorption but do not depend on the "z" coordinate. The density of bulk states is related to the Cr^{3+} ions concentration by absorption coefficient, thus $C_b=I_0(E)\beta(E)Q_b$ where I_0 is the intensity of excitation (number of exciting photons). $C_{si}=N_{si}Q_s$ and N_{s1}, N_{s2} are the concentrations of surface centers at the 1 and 2 surfaces. We have assumed the following solutions of Eq. (2):

$$T(z)=\frac{1}{2\pi}\begin{cases}\phi_1e^{\sigma_1z}, & z<0\\ \displaystyle\int\frac{H(z)e^{ikz}dz}{q(k^2+\sigma_2^2)}+\theta_2e^{-\sigma_2z}+\phi_2e^{-\sigma_2z}, & 0\leqslant z\leqslant L,\\ \theta_3e^{-\sigma_3(z-L)}, & z>L.\end{cases} \tag{5}$$

Considering relations (4) and (5) one obtains

$$\begin{aligned}\int\frac{H(z)e^{ikz}dz}{q(k^2+\sigma_2^2)}=\frac{C_b}{q_2}\Bigg[&\frac{e^{-\beta z}}{\sigma_2^2-\beta^2}+\frac{e^{-\sigma_2z}}{2\sigma_2(\beta-\sigma_2)}\\&+\frac{e^{-\beta L}e^{-\sigma_2(z-L)}}{2\sigma_2(\sigma_2+\beta)}\Bigg]\\&+\frac{1}{2\sigma_2q_2}\lim_{\gamma\to0}[C_{s1}e^{-\sigma_2|z-\gamma|}\\&+C_{s2}e^{-\sigma_2|z-L+\gamma|}].\end{aligned} \tag{6}$$

Conditions for continuity of the temperature function and heat flow at the boundaries allow to calculate ϕ_1,θ_1 and ϕ_2,θ_2. Considering $T_1(0)=T_2(0),T_3(L)=T_4(L)$, $q_1[\partial T_1(z)/\partial z]|_{z=0}=q_2[\partial T_2(z)/\partial z]|_{z=0}$ and $q_2[\partial T_2(z)/\partial z]|_{z=L}=q_3[\partial T_3(z)/\partial z]|_{z=L}$ and assuming that our sample of YAG:Cr^{3+} is thermally opaque ($|\sigma_2|\gg L$) one obtains

$$\theta_2=-\frac{C_b}{2q_2\sigma_2}\frac{1-x}{(\sigma_2+\beta)(1+x)}-\frac{C_{s1}(1-x)}{2q_2\sigma_2(1+x)} \tag{7}$$

and the temperature at the surface at $z=0$

$$T(z=0)=\frac{x}{q_2\sigma_2(1+x)}\left[\frac{C_b}{(\sigma_2+\beta)}+C_{s1}\right], \tag{8}$$

where $x=q_2\sigma_2/q_1\sigma_1$.

Next simplification can be done assuming that $q_2=q_3$ and $\sigma_2=\sigma_3$. Since in our cell the background material is the quartz window and sample is garnet crystal this assumption is quite reasonable. Thus one obtains

$$\phi_2=\frac{-C_be^{-(\sigma_2+\beta)L}}{q_2\sigma_2(\sigma_2+\beta)} \tag{9}$$

and

$$\theta_2=\frac{C_b}{2q_2\sigma_2}\frac{1-x}{(\sigma_2+\beta)(1+x)}-\frac{(C_{s1}+C_{s2}e^{-\sigma_2 L})(1-x)}{2q_2\sigma_2(1+x)}. \tag{10}$$

Finally relations (9) and (10) yield the following formula for the temperature at the surface of the sample:

$$T(z=0)=\frac{-C_b e^{-(\sigma_2+\beta)L}}{2q_2\sigma_2(\sigma_2+\beta)}+\frac{x}{q_2\sigma_2(1+x)}\left[\frac{C_b}{(\sigma_2+\beta)}+C_{s1}+C_{s2}e^{-\sigma_2 L}\right]. \tag{11}$$

To consider the photoacoustic signal quantitatively one has to relate constants C_{si} to C_b.

III. KINETICS OF THE DEEXCITATION

In the following a model of the excitation energy migration from the Cr^{3+} system to the surface is considered. One starts with the optical excitation of the Cr^{3+} system to the state of the energy E via the spin allowed $^4A_2\rightarrow{}^4T_2$ or $^4A_2\rightarrow{}^4T_{1a}$ transitions. In the first step the system relaxes to the metastable state ^2E of the energy E_m [see Fig. 1(b) in paper I]. Next, the excitation of the Cr^{3+} ions can decay radiatively or nonradiatively, or can be transfered to the surface. This process is much slower since is controlled by the metastable state lifetime.

The first fast process yields the fast heat, which is created in a particular Cr^{3+} ion in a place where light has been absorbed. In the next step the excitation can decay radiatively with the rate constant $1/\tau_R$ (τ_R is radiative lifetime) through the spin-forbidden $^2E\rightarrow{}^4A_2$ transition or it can diffuse to the surface with the probability $f(z-z_s)$, where $z-z_s$ is the distance between the Cr^{3+} ion and a surface. Two additional processes take place. The fast nonradiative internal conversion from the higher excited states of the Cr^{3+} directly to the $^4A_2$ electronic manifold and the slow nonradiative internal conversion processes that takes place in the Cr^{3+} system after thermalization in the ^2E state. The third process is the spatial energy transfer between the Cr^{3+} ions. We have not taken this process into account since it is completely reversible process (when a particular Cr^{3+} ion passes the excitation to another Cr^{3+} ion the number of excited Cr^{3+} ions does not change).

The excitation of the Cr^{3+} system is described by following rate equation:

$$\frac{dn_e(z,\omega)}{dt}=I_0(E)\beta(E)e^{-\beta(E)z}(1+e^{i\omega t})-\frac{n_e(z,\omega)}{\tau_e}, \tag{12}$$

where n_e and τ_e are the population and lifetime of the excited state (the bulk states) of energy E, respectively. The rate $1/\tau_e=1/\tau_e^{\rm intra}+1/\tau_e^{\rm inter}$ include the relaxation to the metastable state ^2E, described by lifetime $\tau_e^{\rm intra}$ as well as the interconfigurational internal conversion process, described by $\tau_e^{\rm inter}$. I_0 is intensity of excitation, β is the bulk absorption coefficient, and ω is frequency of excitation modulation. Using the standard methods one can solve Eq. (12) and obtain

$$n_e(z,\omega)=\tau_e I_0(E)\beta(E)e^{-\beta(E)z}\left[1+\frac{e^{i(\omega t+\varphi_e)}}{\sqrt{1+\omega^2\tau_e^2}}\right], \tag{13}$$

where the phase shift is generated by τ_e, $\varphi_e=-\arctan(\omega\tau_e)$. One defines the population of bulk states contributing to the thermal process in the unit time $N_b=n_e/\tau_e$.

Occupation of the metastable ^2E state is given by the following relation:

$$\frac{dn_m(z,\omega)}{dt}=\frac{n_e(z,\omega)}{\tau_e^{\rm intra}}-\frac{n_m(z,\omega)}{\tau_m(z)}. \tag{14}$$

In Eq. (14) the metastable state lifetime τ_m depends on distance of the ion from the surface. Similarly, as in the case of Eq. (12), one obtains

$$n_m(z,\omega)=\tau_m(z)\frac{\tau_e}{\tau_e^{\rm intra}}I_0(E)\beta(E)e^{-\beta(E)z}\times\left[1+\frac{e^{i[\omega t+\varphi_e+\varphi_m(z)]}}{\sqrt{1+\omega^2\tau_m^2(z)}\sqrt{1+\omega^2\tau_e^2}}\right]. \tag{15}$$

In formula (15) the phase related to the lifetime of metastable state is $\varphi_m=-\arctan[\omega\tau_m(z)]$.

We have considered three slow processes that depopulate the metastable state, the radiative $^2E\rightarrow{}^4A_2$ transition, the nonradiative internal conversion process in the Cr^{3+} system related to the $^2E\rightarrow{}^4A_2$ transition and the spatial excitation energy migration. The metastable state depopulation rate can be given as follows:

$$\frac{1}{\tau_m(z)}=\frac{1}{\tau_0}+f(z-z_S), \tag{16}$$

where $f(z-z_s)$ the probability of excitation energy transfer from the Cr^{3+} to the surface. τ_0 is the ^2E state ''local'' lifetime related to the radiative and nonradiative lifetimes as follows: $1/\tau_0=1/\tau_R+1/\tau_{\rm NR}$.

The kinetics equation describing the population of the surface states is given as follows:

$$\frac{dn_s(\omega)}{dt}=\int n_m(z,\omega)f(z-z_s)dz-\frac{n_s(\omega)}{\tau_s}, \tag{17}$$

where τ_s is the lifetime of surface states. Relations (15) and (17) allow one to obtain

$$n_s(\omega)=I_0(E)\beta(E)\frac{\tau_s\tau_e}{\tau_e^{\rm intra}}\left\{\int_0^L e^{-\beta(E)z}\tau_m(z)f(z-z_s)dz+\left[\frac{e^{i(\omega t+\varphi_e+\varphi_s)}}{\sqrt{1+\omega^2\tau_s^2}\sqrt{1+\omega^2\tau_e^2}}\right]\int_0^L e^{-\beta(E)z}\tau_m(z)\times\left[\frac{e^{i\varphi_m(z)}}{\sqrt{1+\omega^2\tau_m^2(z)}}\right]dz\right\}, \tag{18}$$

where the phase shift related to surface states is $\varphi_s = -\arctan(\omega\tau_s)$. We have assumed that the Cr^{3+} ions behave as sensitizer between which the exchange of the excitation can take place and that the sample does not contain any other point defects that behave as activators. Thus the excitation energy, if it is not released in the ion, is passed step by step to the surface. To calculate the probability of such a process we have used the surface quenching model proposed by Flaherty and Powell.[13] According to this approach the probability of transfer of the excitation from the metastable state of the Cr^{3+} ion that is at the distance z from the surface is given by

$$f_R(z) = \frac{1}{\tau_0 \pi}\sqrt{(1-z^2)}\,\arccos\left(\frac{z}{R}\right) \tag{19}$$

for $z \leqslant R$ and zero elsewhere. R is the parameter representing the excitation diffusion (radius of the diffusion) length. Taking into account that we have two surfaces at $z=0$ and $z=L$ we have used the following function:

$$f(z-z_s) = f_R(z) + f_R(z-L). \tag{20}$$

One can see that f_R changes from 0 for $z=R$ to $1/2\tau_0$ for $z=0$. Thus considering relations (20) and (16) one sees that, for the reasonable assumption $2R<L$, $\tau_m(z)$ changes from τ_0 to $\frac{2}{3}\tau_0$. This allows one to use the approximation

$$\left[\frac{\exp[i\varphi_m(z)]}{\sqrt{1+\omega^2\tau_m^2(z)}}\right] \cong \left[\frac{\exp(i\overline{\varphi_m})}{\sqrt{1+\omega^2\overline{\tau_m^2}}}\right],$$

where $\overline{\varphi_m}$ and $\overline{\tau_m}$ are average values of the phase shift and lifetime, respectively. One notices that both the relaxation from the excited state to the metastable state of the Cr^{3+} ion and nonradiative processes at the surfaces are of the order of ns or shorter. Thus considering the time scale of the investigated processes the assumption that $\omega_s\tau_s \ll 1$ and $\omega_s\tau_e \ll 1$ is quite reasonable. As a result one can simplify relation (18) and obtain:

$$n_s(\omega) = \frac{\tau_s\tau_e}{\tau_e^{\text{intra}}} I_0(E)\beta(E)\left[1+\frac{e^{i(\omega t+\overline{\varphi_m})}}{\sqrt{1+\omega^2\overline{\tau_m^2}}}\right] \times \int_0^L e^{-\beta(E)z}\tau_m(z) f(z-z_s)\,dz, \tag{21}$$

where according to Eq. (19)

$$\int_0^L e^{-\beta(E)z}\tau_m(z) f(z-z_s)\,dz = \frac{R}{\pi}\left[\int_0^L \frac{e^{-\beta(E)Rx}\sqrt{1-x^2}\arccos(x)}{1+\frac{1}{\pi}\sqrt{1-x^2}\arccos(x)}\,dx + e^{-\beta(E)L}\int_0^L \frac{e^{\beta(E)Rx}\sqrt{1-x^2}\arccos(x)}{1+\frac{1}{\pi}\sqrt{1-x^2}\arccos(x)}\,dx\right], \tag{22}$$

where $x = z/R$.

One can calculate both integrals for different values of the product βR. In the case of the samples doped with Cr^{3+} we deal with weak absorption. Thus one can use the assumptions $\beta R \ll 1$ and $\exp(-\beta R x) \cong 1$, even if the migration distance R is comparable with sample thickness L. Similarly like in the case of estimation of average lifetime $\overline{\tau_m}$ one can approximate

$$\frac{1}{1+\pi^{-1}\sqrt{1+x^2}\arccos(x)} \cong \frac{4}{5}.$$

Than considering that $\int_0^1 \sqrt{1+x^2}\arccos(x)\,dx = \frac{1}{4} + \pi^2/16$ one obtains

$$\int_0^L e^{-\beta(E)z}\tau_m(z) f(z-z_s)\,dz \cong \frac{R}{5}\left[\frac{1}{\pi}+\frac{\pi^2}{4}\right](1+e^{-\beta(E)L}). \tag{23}$$

Finally the number of surface states that contribute to the heat released at the front and back surface in the unit time is given by

$$\frac{n_s(z,\omega)}{\tau_s} = N_{s1}\delta(z) + N_{s2}\delta(z-L) = I_0(E)\beta(E) \times \frac{R}{5}\left[\frac{1}{\pi}+\frac{\pi^2}{4}\right][\delta(z)+\delta(z-L)e^{-\beta(E)L}] \times \left[1+\frac{e^{i\omega t+i\overline{\varphi_m}}}{\sqrt{1+\omega^2\overline{\tau_m^2}}}\right]\frac{\tau_e}{\tau_e^{\text{intra}}}. \tag{24}$$

IV. PAS SIGNAL IN THE CASE YAG:Cr^{3+} SYSTEM

The relation between the coefficients C_b and C_{si} can be calculated when we consider that the surface states behave as activators that obtain excitation via the sensitizing Cr^{3+} ions. Considering Eqs. (24) and (11) one obtains the following relations:

$$C_b = I_0(E)\beta(E)Q_b, \tag{25}$$

$$C_{s1} = C_b\frac{\tau_e}{\tau_e^{intra}}[\sigma_2+\beta(E)]\frac{R\sigma_2}{5}\left[\frac{1}{\pi}+\frac{\pi^2}{4}\right]\left[\frac{e^{-i\overline{\varphi_m}}}{\sqrt{1+\omega^2\overline{\tau_m^2}}}\right]\frac{Q_s}{Q_b},$$

$$C_{s2} = C_{s1}e^{-[\sigma_2+\beta(E)]L}.$$

For an optically thin sample, where $|\sigma_2| \gg \beta$ relation (11) can be presented in the form

$$T(z=0) = \frac{x}{q_2\sigma_2^2(1+x)} I_0(E)\beta(E)\left[Q_b + \frac{R\sigma_2}{5}\left[\frac{1}{\pi}+\frac{\pi^2}{4}\right] \times \frac{(1+e^{-\sigma_2 L})e^{-i\overline{\varphi_m}}}{\sqrt{1+\omega^2\overline{\tau_m^2}}}\,\frac{\tau_e}{\tau_e^{\text{intra}}}Q_s\right]. \tag{26}$$

Since $\sigma_2 = (1+i)\sqrt{\omega/2\alpha_2}$, the above relation yields

$$T(z=0)=\frac{x}{q_2\sigma_2^2(1+x)}I_0(E)\beta(E)\times\left[Q_b+K_0\sqrt{\omega}\frac{(1+e^{-\sigma_2 L})e^{-i(\bar{\varphi}_m-\pi/4)}}{\sqrt{1+\omega^2\bar{\tau}_m^2}}\frac{\tau_e}{\tau_e^{\text{intra}}}Q_s\right], \tag{27}$$

where K_0 is a real quantity:

$$K_0=\frac{R}{5\sqrt{2\alpha_2}}\left[\frac{1}{\pi}+\frac{\pi^2}{4}\right]. \tag{28}$$

One can see that product $R\sigma_2$ yields an additional phase shift equal to $-\pi/4$ for the thermal signal generated at the surface. As will be discussed later this effect influences the total PAS phase quite strongly.

Since the energy migration is the energy conserving process, the heat released after migration at the surface $Q_s=E_m$, where E_m is energy of the ^2E state of the Cr^{3+} ion. When the isolated Cr^{3+} ion has a 100% quantum efficiency the heat released in the bulk by the excited Cr^{3+} ion $Q_b=E-E_m$, where E is the excitation energy. It is the heat emitted immediately after excitation in the Cr^{3+} place. It is easy to extend the model to include the effect of nonradiative relaxation inside the Cr^{3+} system. In this case

$$Q_b=E-E_m+P_{\text{NR}}^e(E)E_m+[1-P_{\text{NR}}^e(E)]P_{\text{NR}}^m E_m\frac{(1+e^{-\sigma_2 L})e^{-i\tilde{\varphi}_m}}{1+\omega^2\bar{\tau}_m^2}, \tag{29}$$

where $P_{\text{NR}}^e(E)=\tau_e/\tau_e^{\text{inter}}=1-\tau_e/\tau_e^{\text{intra}}$ is the probability of the fast internal conversion processes in the excited vibronic states of the ^2E, $^4T_2$, and $^4T_{1a}$ electronic manifolds (this probability depends on the excitation energy), P_{NR}^m is probability of nonradiative internal conversion of the Cr^{3+} system after termalization in the ^2E state (this probability depends on temperature). As a consequence of consideration of the fast internal conversion processes in the excited states occupation of the metastable state is reduced by factor of $(1-P_{\text{NR}}^e)$. Total nonradiative energy conversion quantum efficiency of the isolated Cr^{3+} η_{NR}, defined by Eq. (6) in paper I can be related to P_{NR}^e and P_{NR}^m. Using a diabatic model[15] of nonradiative relaxation one obtains

$$\eta_{\text{NR}}=1-\eta_R=1-(1-P_{\text{NR}}^e)(1-P_{\text{NR}}^m). \tag{30}$$

One can easy see that relation (30) allows that $P_{\text{NR}}^e+P_{\text{NR}}^m>1$. Since the quantity that is analyzed is the PAS of the sample divided by the PAS obtained from excitation of carbon reference material one obtains the complex PAS signal

$$Q_{\text{PAS}}\propto\beta(E)\left[\frac{E-E_m}{E}+K\frac{E_m}{E}\right]. \tag{31}$$

Here the complex coefficient K is given as

$$K=P_{\text{NR}}^e+(1-P_{\text{NR}}^e)P_{\text{NR}}^m\frac{(1+e^{-\sigma_2 L})e^{-i\bar{\varphi}_m}}{\sqrt{1+\omega^2\bar{\tau}_m^2}}+(1-P_{\text{NR}}^e)K_0\sqrt{\omega}\frac{(1+e^{-\sigma_2 L})e^{-i(\bar{\varphi}_m-\pi/4)}}{\sqrt{1+\omega^2\bar{\tau}_m^2}}. \tag{32}$$

The amplitude of PAS is given as

$$Q_{\text{PAS}}=\beta(E)\sqrt{\left[\frac{E-E_m}{E}+\text{Re}(K)\frac{E_m}{E}\right]^2+\left[\text{Im}(K)\frac{E_m}{E}\right]^2}, \tag{33}$$

where $\text{Re}(K)$ and $\text{Im}(K)$ are the real and imaginary parts of the K coefficient. One can analyze the quantity

$$\frac{d}{dE}\left[\frac{Q_{\text{PAS}}(E)}{\beta(E)}\right]=\frac{E_m}{E^2}\frac{\{E+[\text{Re}(K)-1]E_m\}[1-\text{Re}(K)]-[\text{Im}(K)]^2E_m}{\sqrt{[E-E_m+\text{Re}(K)E_m]^2+[\text{Im}(K)E_m]^2}}. \tag{34}$$

$\{E+[\text{Re}(K)-1]E_m\}[1-\text{Re}(K)]-[\text{Im}(K)]^2E_m>0$ corresponds to an increase of the ratio of the Q_{PAS} to the absorption coefficient, whereas $\{E+[\text{Re}(K)-1]E_m\}[1-\text{Re}(K)]-[\text{Im}(K)]^2E_m<0$ yields the decreasing of the ratio of Q_{PAS} to absorption, with increasing excitation energy. Considering the $Q_{\text{PAS}}(E)/\beta(E)$ for different excitation energy one obtains information on the nonradiative processes that take place in the system. Quantity $Q_{\text{PAS}}(E)/\beta(E)$ calculated using our model for different values of parameters is presented in Fig. 2. In all cases the $Q_{\text{PAS}}(E)/\beta(E)$ has been normalized to the quantity obtained for $E-E_m=100\ \text{cm}^{-1}$. It is quite an arbitrary choice that has been taken because it allows one to present the results as not crossing curves. In fact we are interested in the slope not in absolute value of $Q_{\text{PAS}}(E)/\beta(E)$. The curves in Fig. 2(a) have been obtained under assumption $P_{\text{NR}}^e=0$ and correspond to different K_0, indicated in figure, and to two limit values of P_{NR}^m, zero and unity. Quantity of the ratio of PAS amplitude to absorption for other values of P_{NR}^m should be placed between the limit curves. In Fig. 2(b) the $Q_{\text{PAS}}(E)/\beta(E)$ has been obtained for nonzero values of P_{NR}^e. We have considered that the probability of internal conversion process in the higher vibronic states of excited electronic manifolds are described by diabatic model.[15] We have approximated results of the model using an analytical function. Thus

$$P_{\text{NR}}^e(E)=b\frac{e^{-E_{\text{NR}}/(E-E_m)}}{1+be^{-E_{\text{NR}}/(E-E_m)}}. \tag{35}$$

Here E_{NR} is the characteristic energy barrier for nonradiative processes (this energy is related to the energy of the ground and excited electronic manifold crossover) and b is the relative frequency factor describing the probability of the internal conversion with respect to the probability of intraconfigurational relaxation. For performing calculations we have

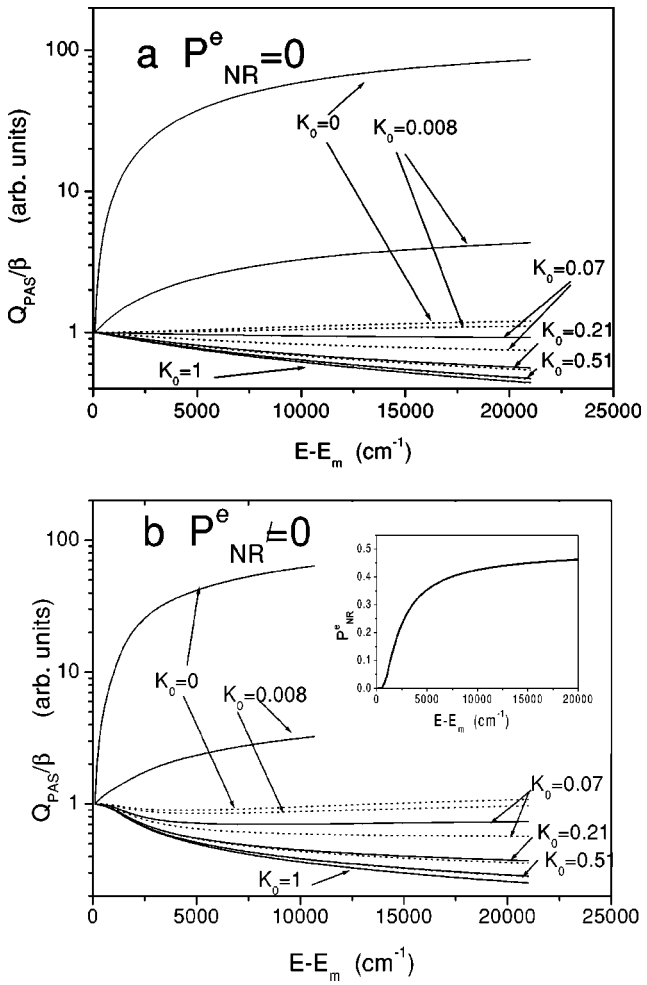

FIG. 2. Dependence of the ratio of photoacoustic signal to the absorption on excitation energy for different values of K_0. Solid curves have been obtained assuming $P^m_{\mathrm{NR}}=0$, dashed curves have been obtained for $P^m_{\mathrm{NR}}=1$. (a) Curves obtained assuming $P^e_{\mathrm{NR}}=0$, (b) curves obtained for $P^e_{\mathrm{NR}}\neq 0$, quantity K_0 is given in $\mathrm{s}^{-1/2}$ units.

assumed $E_{\mathrm{NR}}=3000\ \mathrm{cm}^{-1}$ and $b=1$. The shape of this function is presented in the inset of Fig. 2(b).

Actually we have measured the ratio of the amplitude of PAS to the absorption coefficient in the region of the $^4A_2\rightarrow{}^4T_2$ absorption band and in the region of $^4A_2\rightarrow{}^4T_{1a}$ absorption band of the Cr^{3+} ion. One defines the quantity

$$\gamma=\frac{Q_{\mathrm{PAS}}(^4A_2\rightarrow{}^4T_{1a})}{\beta(^4A_2\rightarrow{}^4T_{1a})}\,\frac{\beta(^4A_2\rightarrow{}^4T_2)}{Q_{\mathrm{PAS}}(^4A_2\rightarrow{}^4T_2)}. \qquad (36)$$

Quanity γ is presented in Fig. 3 versus frequency of excitation. One can consider some special cases. In absence of the spatial energy migration ($K_0=0$) and nonradiative internal conversion ($P^e_{\mathrm{NR}}=0$ and $P^m_{\mathrm{NR}}=0$) one obrtains

$$\gamma=\frac{E(^4A_2\rightarrow{}^4T_2)}{E(^4A_2\rightarrow{}^4T_{1a})}\,\frac{E(^4A_2\rightarrow{}^4T_{1a})-E_m}{E(^4A_2\rightarrow{}^4T_2-E_m)}.$$

For YAG:Cr^{3+}, where $E(^4A_2\rightarrow{}^4T_2)=16\,670\ \mathrm{cm}^{-1}$, $E(^4A_2\rightarrow{}^4T_{1a})=22\,830\ \mathrm{cm}^{-1}$, and $E_m=14\,450\ \mathrm{cm}^{-1}$, this

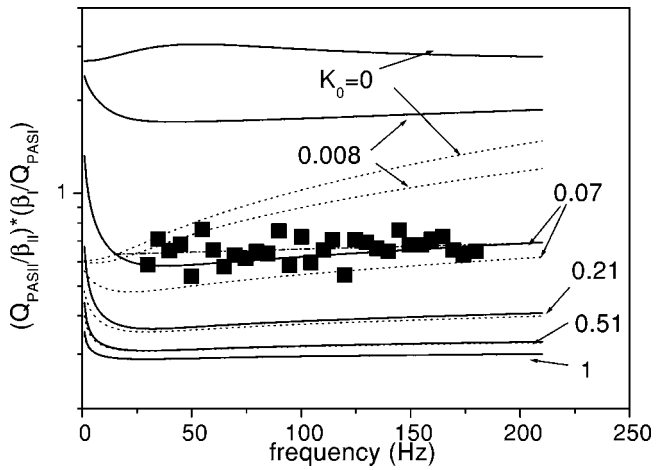

FIG. 3. Quantity γ [see Eq. (36)] versus excitation frequency calculated for different value K_0, solid curves correspond to $P^m_{\mathrm{NR}}=0$, dashed curves have been obtained for $P^m_{\mathrm{NR}}=1$, rectangles represent the experimental values, and the dot-dashed line is a linear fit to the experimental data, quantity K_0 is given in $\mathrm{s}^{-1/2}$ units.

ratio would be equal to 2.76. The second limit case is when the excitation can migrate through all volume of the sample. This corresponds to $K_0=\infty$. For YAG:Cr^{3+} one would obtain $\gamma=E(^4A_2\rightarrow{}^4T_2)/E(^4A_2\rightarrow{}^4T_{1a})=0.73$, independently of P^m_{NR} for any $P^e_{\mathrm{NR}}<1$. It is seen from Fig. 3 that experimental ratio is of the order of 0.5–0.6. We have performed calculations of ratio γ using formula (31) with K defined by relation (32). Already we have considered that the ^2E state of the Cr^{3+} system is much better excited via the $^4A_2\rightarrow{}^4T_2$ transition than $^4A_2\rightarrow{}^4T_{1a}$ transition. The analysis of the excitation spectra presented in Fig. 4(c) (paper I) allows one to consider that probability P^e_{NR} is equal 0 and 0.63 for excitation via the $^4A_2\rightarrow{}^4T_2$ and $^4A_2\rightarrow{}^4T_{1a}$ transitions, respectively (or more generally, the ratio $[1-P^e_{\mathrm{NR}}(^4A_2\rightarrow{}^4T_2)]/[1-P^e_{\mathrm{NR}}(^4A_2\rightarrow{}^4T_{1a})]=\frac{1}{0.37}$) . We have calculated quantity γ keeping parameter P^e_{NR} fixed 0 and 0.63, for respective transitions, and treating the quantities K_0 and P^m_{NR} as fitting parameters. The results of calculations are presented in Fig. 3. The solid curves correspond to the data obtained assuming that we have not the nonradiative internal conversion in the Cr^{3+} after termalization in the ^2E state ($P^m_{\mathrm{NR}}=0$). The dashed curves have been obtained under assumption that dominant internal relaxation in the Cr^{3+} system is nonradiative ($P^m_{\mathrm{NR}}=1$). It is of course not true because we have the $^2E\rightarrow{}^4A_2$ luminescence, but similar Figs. 2(a) and 2(b), curves obtained for $P^m_{\mathrm{NR}}=0$ and $P^m_{\mathrm{NR}}=1$ represent the limit cases and all other value of P^m_{NR} parameter should be represented by the functions with values between them.

One should notice that there are two effects diminishing the quantity γ: the energy migration to the surface and the dependence of the probability of fast nonradiative internal conversion P^e_{NR} on excitation energy. Since the probability of nonradiative internal conversion process in the excited states of the Cr^{3+}, P^e_{NR}, is known our model allows estimating the

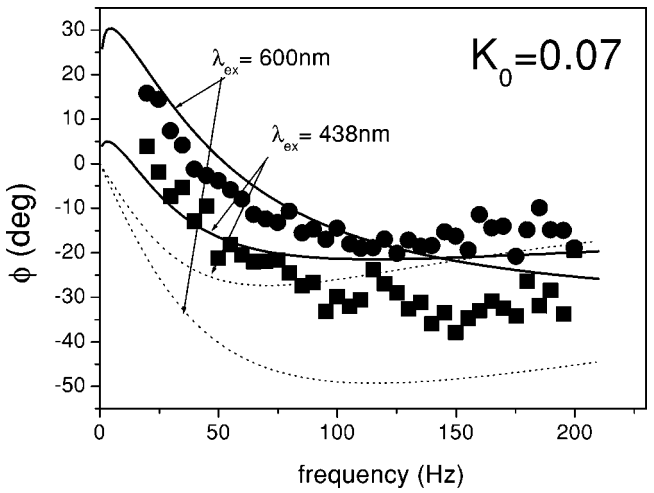

FIG. 4. Dependence of PAS phase on excitation frequency. Dots correspond to the experimental data obtained under excitation with 600 nm, rectangles correspond to the experimental data obtained under excitation with 438 nm. Dashed curves have been obtained using the basic model, solid curves have been obtained using our model (see the text), quantity K_0 is given in $s^{-1/2}$ units.

quantity K_0, the constant that describes the energy migration from Cr^{3+} to the surface. The estimated value was $K_0 = 0.07\ s^{-1/2}$. Considering that the thermal diffusivity of the garnet is $\alpha_2 = 3.66 \times 10^{-2}\ cm^{-2}/s$ and the corresponding migration radius is $R = 0.034$ cm. One can see that for $K_0 > 0.07\ s^{-1/2}$ the difference between curves corresponding to $P^m_{NR} = 0$ and $P^m_{NR} = 1$ are negligible. This is a reason why we cannot estimate the total quantum efficiency of the Cr^{3+} ion from this analysis. We have used our model and analyzed the frequency dependence of the PAS phase. The experimental results are presented in Fig. 4. The phase of the PAS has been measured under excitation with 600 and 438 nm, which correspond to the excitation via $^4A_2 \rightarrow {}^4T_2$ and $^4A_2 \rightarrow {}^4T_{1a}$ transitions, respectively, and calibrated with respect to the glassy carbon. The phase has been calculated according to the formula

$$\Phi = -\arctan\left[\frac{\mathrm{Im}(K)E_m}{[E - E_m + \mathrm{Re}(K)E_m]}\right], \tag{37}$$

where the K coefficient is defined by Eq. (32). We have compared the results of our model with predictions of the model suggested by Quimby and Yen[16] and Mandelis *et al.*,[17] for analysis of the quantum efficiency of ruby crystal. This model does not include the nonradiative internal conversion in the higher excited states described in our model by quantity P^e_{NR} and spatial energy migration described by constant K_0. Further we refer to the latter as a basic model. One can see that the experimental phase shift is quite large, which may suggest the weak quantum efficiency of the YAG: Cr^{3+} system. To reproduce more or less the experimental data with the basic model one should make the assumption that the Cr^{3+} is an almost nonradiative center. In Fig. 4 the phase shifts calculated according basic model with quantum efficiency equal zero are represented by dashed curves. One can see that the basic model reproduces the experimental data quite well obtained when the excitation with 438 nm is considered, and the reproduction is bad when the excitation with 600 nm is considered. Experimentally the PAS phase for excitation 600 nm is more positive than under excitation 438 nm, whereas the basic model yields an opposite effect. We have reproduced the phase shift using our model quite well. The theoretical dependence of PAS phase on frequency of excitation obtained for $K_0 = 0.07\ s^{-1/2}$ for P^m_{NR} equal to 0 are presented in Fig. 4. In both cases the fitting is not bad. Specifically our model reproduces the proper phase difference between PAS excited with 600 and 438 nm. In addition our experimental phase shifts show the existence of an additional phase shift $-\pi/4$ induced by the effect of energy migration. Our fitting to the PAS phase has been the best when we have assumed a high local quantum efficiency of Cr^{3+}. This is expected since in YAG we deal with a high field material characterized by strong R line luminescence.

V. CONCLUSIONS

We have extended the standard theory of photoacoustic-photothermal processes by considering the spatial migration of excitation energy in solids. Specifically we have considered the transport of the excitation from the Cr^{3+} center to the surface states. As far as the qualitative theoretical results are considered we have obtained the final formulas that relate PAS to optical absorption given by relations (31) and/or (33). Actually these formulas are already known to describe systems characterized by two step deexcitations. As an example one can mention the paper by Oufaze *et al.*,[18] where the PAS signal from a molecular system have been discussed. One can consider relation (31) in a quite general way. If $K = 0$ we deal with a completely radiative center. The quantum efficiency of the system is 100%. In such a case the PAS is generated due to the fast nonradiative process in higher excited states of the system. If $K = 1$ the PAS follows (is proportional to) the absorption. It is equivalent to the case when all energy is transformed into heat without delay. No phase shift of PAS related to the ''long living'' excited metastable states in the system is noticed. This is the case where we can use the Rosencwaig-Gersho,[1] approach without any modifications.

The interesting implication of the present extension of the theory of photoacoustic effect is that in the case of existence of nonradiative transfer from the localized absorbing center to the surface the coefficient $|K|$ can be much greater than unity. This is because only the Cr^{3+} ions from the layer thinner than thermal diffusion length can contribute directly to the PAS whereas all the Cr^{3+} ions that are placed at distance R from the surface contribute to the PAS coming from the surface. This is the main reason for the nontrivial effect of diminishing the ratio of PAS to absorption coefficient with increasing excitation energy. However, the decrease of the ratio of the PAS amplitude to absorption coefficient with increasing of excitation energy can also be caused by respective increasing of the probability of fast nonradiative internal conversion. The latter effect emerges when a change in probability of internal conversions yields the change of the PAS phase. In this paper we have particularly discussed the case

of the YAG:Cr^{3+} system, with chromium concentration 2×10^{20} cm^{-3}. We have found that in our system the excitation energy migration from chromium to surface states is the main effect responsible for PAS generation. Using our model we have estimated the local quantum efficiency of the system. Specifically we have found that the probability of nonradiative internal conversion of the system thermalized in the ^2E state is very small, $P^m_{NR}\cong 0$. Thus the quantum efficiency of the Cr^{3+} excited via $^4A_2\rightarrow{}^4T_2$ is equal to 100%. There is a different situation where the system is excited via the $^4A_2\rightarrow{}^4T_{1a}$ transition. Since in this case the probability of the internal conversion in the excited states is $P^e_{NR}=0.63$ the quantum efficiency of the Cr^{3+} ion defined by relation $(1-P^e_{NR})(1-P^m_{NR})$ is equal 37%. This is a reason why the basic model[16,17] can reproduce the dependence of the PAS phase excitation frequency for excitation with 438 nm . The basic model fails when we excite with wavelength 600 nm in the region of the $^4A_2\rightarrow{}^4T_2$ transition when the quantum efficiency of the Cr^{3+} is high.

We can relate the isolated Cr^{3+} ion quantum efficiency to the quantum efficiency of all the systems. Our analysis of the ^2E state radiative and nonradiative deexcitation [formulas (16) and (19)] showed that depending on diffusion length R up to 1/3 of the excited ions can transfer their energy to the surface. This means that the quantum efficiency of the entire system can be diminished by factor 2/3, actually independently of the local quantum efficiency.

Let us consider the example of ruby crystal, for which many reports on quantum efficiency is available in literature. The energetic structure of the Cr^{3+} ion in Al_2O_3 lattice (very high field material with the energy of $^4T_2$ far above ^2E) allows assuming that it is pure radiative center characterized by quantum efficiency very close to 100%. The ^2E state is characterized by very weak electron-lattice coupling, thus according to the diabatic model,[15] also presented in paper I, the probability of fast nonradiative internal conversion processes in this system is very small. On the other hand, the entire system (Cr^{3+} and lattice) can be characterized by the spatial excitation energy migration from the ion to the surface and nonradiative relaxation through the surface states. This causes the final quantum efficiency of the system to be smaller than 100%. According to the above remarks the quantum efficiency of all the system can be diminished from 100 to 66.(6) %.

There are two methods that allow one to determine quantum efficiency. The direct one is optical based on the estimation of the ratio of emitted to absorbed photons.[19] This method does not allow one to distinguish between different nonradiative processes. It is interesting that in some cases the quantum efficiency of ruby crystal obtained using the pure optical approach is quite small and close to the limit 66.(6)% obtained by us [63%,[19] 65%[20] and 78% (Ref. 21). Such a low quantum efficiency can be related to the effect of nonradiative energy transfer to the surface states.

The indirect method of estimation quantum efficiency is based on the analysis of the dependence of PAS on frequency.[12] This method allows one to estimate the quantum efficiency based on the nonradiative processes only. Moreover as has been shown in this paper the photoacoustic method allows one to distinguish between local nonradiative processes and energy migration processes. For the case of the ruby system the quantum efficiency estimated using photoacoustic/photothermal methods has been larger [90%,[16] 90–98% (Ref. 17)]. It should be mentioned that the experimental results presented in Refs. 16 and 17 allow one to exclude the existence of the spatial excitation energy migration in the samples under consideration. Based on the above considerations the general conclusions that the photoacoustic method is a very powerful tool for investigation of nonradiative processes in the luminescence centers and studying energy migration in the complex systems can be formulated.

ACKNOWLEDGMENTS

This paper has been supported by the Polish Committee for Scientific Research (Grant No. 7T07B049 18).

[1] A. Rosencwaig and A. Gresho, J. Appl. Phys. **47**, 64 (1976).
[2] M. Grinberg, A. Sikorska, A. Sliwinski, J. Barzowska, Y.R. Shen, S.B. Ubizskii, and S.S. Melnyk, Phys. Rev. B (preceding paper), Phys. Rev. B **67**, 045113 (2003).
[3] D.L. Dexter J. Chem. Phys. **21**, 836 (1953).
[4] M. Inokuti and F. Hirayama, Phys. Rev. **43**, 1978 (1965).
[5] M. Yokota and O. Tamimoto, J. Phys. Soc. Jpn. **22**, 779 (1967).
[6] M.J. Weber, Phys. Rev. B **4**, 2932 (1971).
[7] S.R. Rotman and F.X. Hartman, Chem. Phys. Lett. **152**, 391 (1988).
[8] O. Barbosa-Garcia and C.W. Struck, J. Chem. Phys. **100**, 4554 (1994).
[9] D. Pines and D. Huppert, Isr. J. Chem. **29**, 473 (1989).
[10] K. Tonooka, N. Kamata, K. Yamada, K. Matsumoto, and F. Maruyama, J. Lumin. **50**, 139 (1991).
[11] S.G. Fedorenko, A.I. Burshtein, and A.A. Kipriyanov, Phys. Rev. B **48**, 7020 (1993).
[12] R.S. Quimby and W.M. Yen, J. Appl. Phys. **51**, 4985 (1980).
[13] J.M. Flaherty and R.C. Powell, Phys. Rev. B **19**, 32 (1979).
[14] J.C. Murphy, L.C. Aamodt, and J.W.M. Spicer, in *Principles and Perspectives of Photothermal and Photoacoustic Phenomena*, edited by A. Mandelis (Elsevier, New York, 1992), p. 41.
[15] M. Grinberg and A. Mandelis, Phys. Rev. B **49**, 12 496 (1994).
[16] R.S. Quimby and W.M. Yen, J. Appl. Phys. **51**, 1780 (1980).
[17] A. Mandelis, M. Munidasa, and A. Othonos, IEEE J. Quantum Electron. **29**, 1498 (1993).
[18] M. Oufaze, P. Poulet, and J. Chambron, Photochem. Photobiol. **55**, 491 (1992).
[19] F. Castelli and L.S. Forster, J. Lumin. **8**, 252 (1974).
[20] E.E. Burke and Z.L. Morgenshtern, Opt. Spectrosc. **14**, 362 (1963).
[21] A. Misu, J. Phys. Soc. Jpn. **19**, 2260 (1964).